

PROJECT REPORT ON
***IONOSPHERIC TEC PERTURBATIONS DUE TO POSSIBLE TSUNAMI WAVES
FOLLOWING THE DECEMBER 26th, 2004 SUMATRA EARTHQUAKE***

SUBMITTED BY

ABHIJEET TRIPATHY

M.Sc. Applied Geophysics, IIT Bombay



STUDY AND WORK CARRIED UNDER THE GUIDANCE OF

Dr.S.SRIPATHI

INDIAN INSTITUTE OF GEOMAGNETISM

New Panvel, Navi Mumbai



CONTENTS

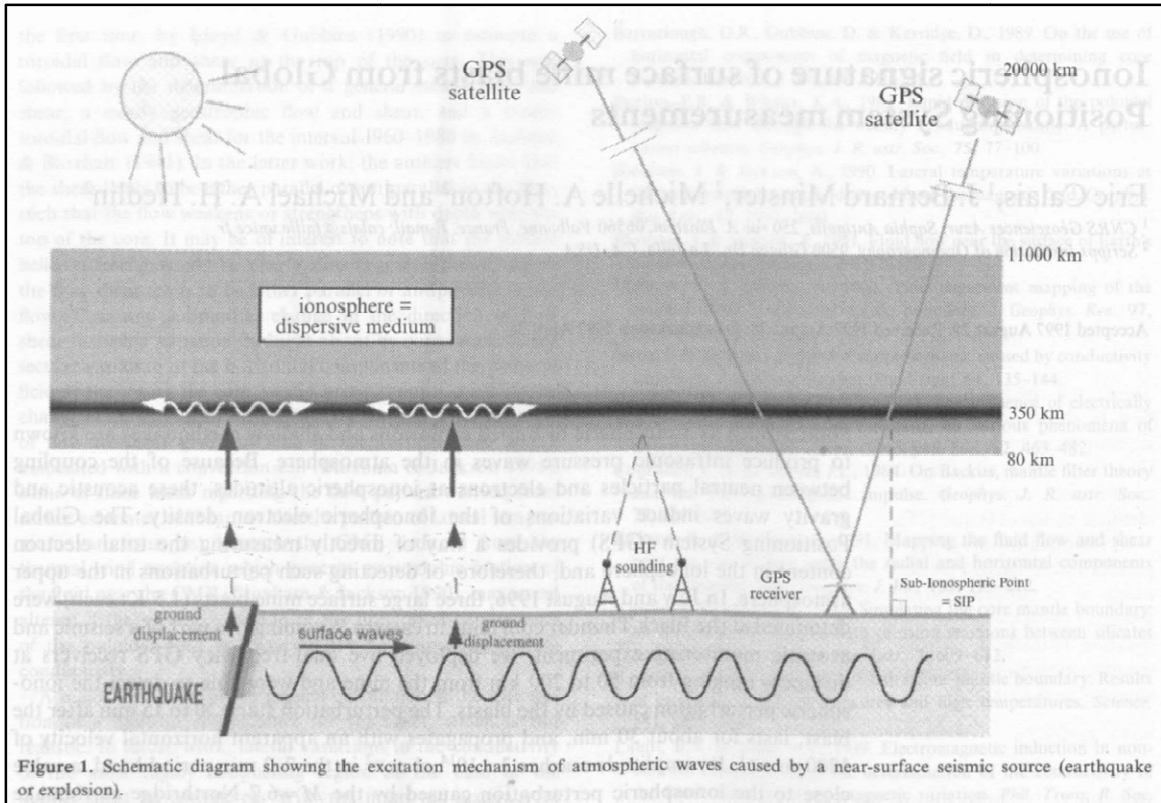
INTRODUCTION	5-16
DATA	16-17
METHODOLOGY	17-21
RESULT AND DISCUSSION	22
CONCLUSION	22
REFERENCES	23

INTRODUCTION

Natural hazards, including earthquakes, volcanic eruptions, and tsunamis, have been significant threats to humans throughout recorded history. The Global Positioning System (GPS) satellites have become primary sensors to measure signatures associated with such natural hazards. These signatures typically include GPS-derived seismic deformation measurements, co-seismic vertical displacements. Another way to use GPS observables is to compute the ionospheric total electron content (TEC) in order to detect ionospheric disturbances caused by earthquakes, volcano eruptions, and tsunamis. There are various natural sources that could generate atmospheric pressure waves that could travel in lower atmosphere and will also propagate in upper atmosphere and even to the ionosphere. Among these sources, atmospheric pressure waves from earthquake had been rarely observed hence less well known before the Alaska earthquake ($M_w=9.0$) of 1964, except a few observations of early short period sound waves as well as air waves coupled with seismic surface waves. Since that time, a large number of observations on atmospheric waves related to earthquake sources have been reported. These observations include 4 different types of atmospheric waves:-

- Low frequency acoustic-gravity waves produced from the source region and propagated directly through the lower atmosphere to long distance.
- Medium to higher frequency infrasonic waves which are radiated also from the source and sometimes converted into somewhat different forms such as reflected or diffracted waves from earth's topography during their propagation path.
- Infrasonic waves coupled with large amplitude seismic Rayleigh waves during their passage through observation sites along the ground surface.
- Atmospheric gravity waves induced by tsunami waves that are generated from large earthquakes.

Tsunamis are long surface gravity waves that propagate for great distances in the ocean. They are usually triggered by submarine earthquakes, landslides or eruptions. While tide gauges can measure tsunami waves along the coast,



detection and monitoring in the open ocean is very challenging due to the long wavelengths (typically 200 km) and small amplitudes (a few cm or less of sea surface vertical displacement) compared to wind-generated waves. Reported offshore detections involve ocean-bottom sensors (pressure gauges or seismometers), sea level measurement from Global Positioning System receivers on buoys or satellite altimetry.

Since the 1960s, numerous observations of acoustic-gravity waves in the ionosphere induced by solid Earth events, such as earthquakes, mine blasts or explosions, have been published (Bolt 1964; Harkrider 1964; Calais et al. 1998). They highlighted the generation of such atmospheric waves at the Earth surface by vertical displacements with very small amplitude but large wave length, such as seismic surface waves. The main reason for having such coupled solid-Earth atmosphere signals is that the exponential decrease of density with height causes an exponential amplification of the atmospheric wave by conservation of the

kineticEnergy.

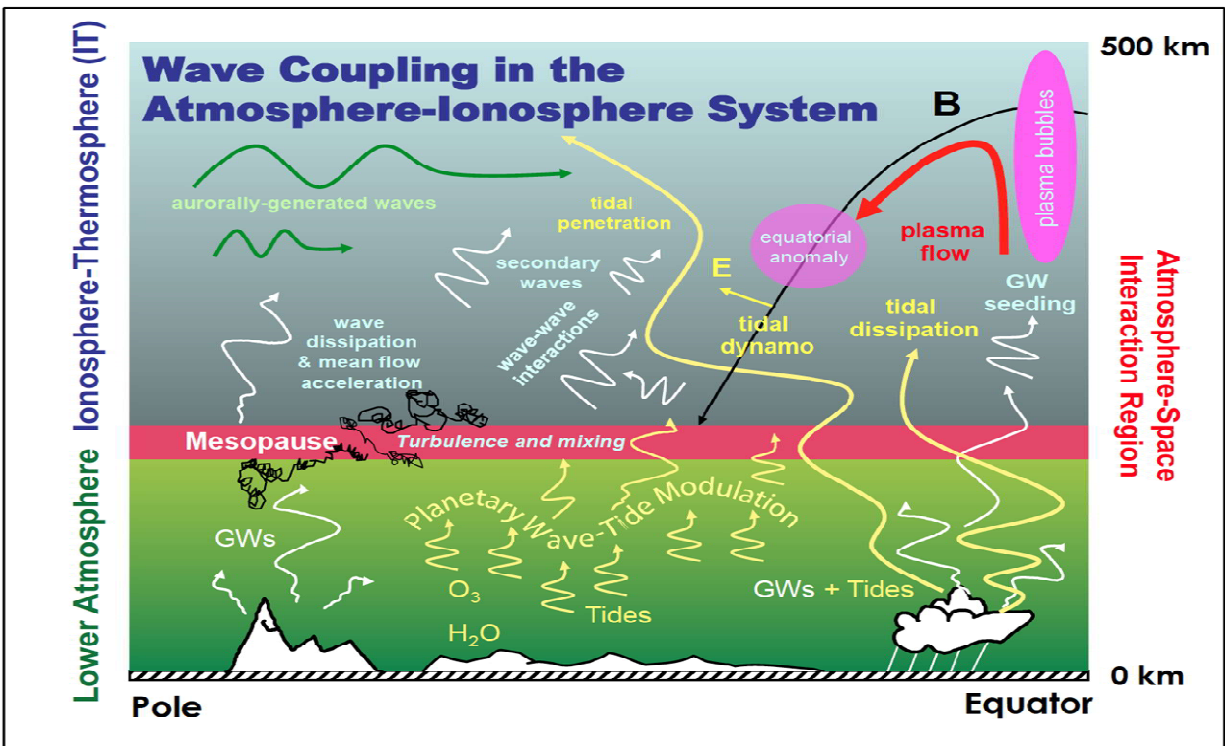
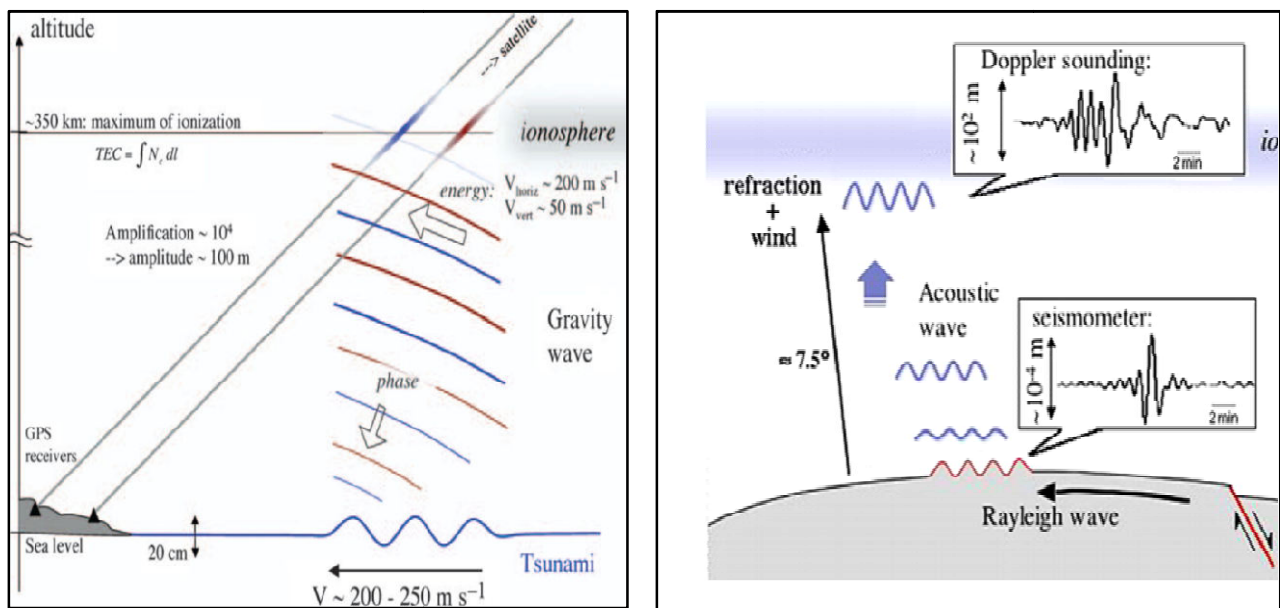


Fig. The primary mechanism through which energy and momentum are transferred from the lower atmosphere to the ionosphere is through the generation and propagation of waves.

In the F region of the ionosphere (150–600 km of altitude), the velocity perturbation is typically amplified by a factor of 10^4 compared to the ground velocity, and is therefore detectable on ground-based or ground-satellite measurement.

Tsunami waves are expected to induce a similar type of coupling with the atmosphere, despite their small amplitude compared to ocean swell, they can generate atmospheric gravity waves because of their long wavelengths. The possibility of detection of tsunamis by monitoring the ionospheric signature of the induced gravity wave was proposed by Peltier & Hines (1976). They discussed the theoretical issue of the coupling, and found that the several difficulties one would expect a priori should not have any major consequences on the feasibility. Part of the problem is certainly the lack of ionospheric measurements above the oceans, and also the difficulty to distinguish tsunami-related gravity waves from any other source of traveling ionospheric disturbances.

More recently, the development of high-density Global Positioning System (GPS) networks have made a breakthrough in ionospheric monitoring, allowing us to image propagation of Traveling Ionospheric Disturbances (TIDs) over large areas. The detection and imaging of Rayleigh waves after the 2002 Denali earthquake using California GPS networks (Ducic et al. 2003) showed that despite the fact that GPS measures the integrated electron density between the satellite and the receiver, small scale waves could be resolved and identified using adepated data processing. Moreover, the geometry of GPS ionospheric measurements is particularly interesting for the detection of offshore signal: as the maximum of sensitivity is obtained in the F region along the satellite-receiver rays, GPS receivers on coastal areas will provide coverage off shore, up to several hundred kilometres away from the coast.



Figs. Schematic view of our study. The geometry of GPS measurements allows to detect ionospheric perturbations above the open ocean, and therefore possible gravity waves induced by earthquake/tsunamis.

IONOSPHERE LAYERS

The Ionosphere is a layer of the upper atmosphere where some of the electrons

have been removed from the atoms and molecules to form free electrons and positively charged ions. The most common way happened is by extreme ultraviolet light from the sun separating a single electron from an oxygen atom. The maximum ionization takes place near a height of about 300km (about 200 miles). Only one part in a thousand of the material is ionized here. Most of the gas remains electrically neutral. The presence of the electrons which are free to move alters the speed that electromagnetic waves travel. One well known effect of the ionosphere is the bending of the shortwave radio transmissions, so that it is possible to receive signals from stations that are over the horizon.

The ionosphere is contained in the uppermost layers of the earth's atmosphere where most of the earth-bound ultraviolet light and atomic particles emitted by the sun are absorbed. This region of free electrons and ionized atoms fluctuates with solar activity and under severe conditions has interrupted communications and electrical power over wide areas. The ionosphere also has a severe impact on the signals from the GPS satellites, as well as millions of other users employ for positioning and navigation.

For convenience, we divide the Ionosphere into four broad regions called D, E, F, and topside. These regions may be further divided into several regularly occurring layers, such as F1 or F2.

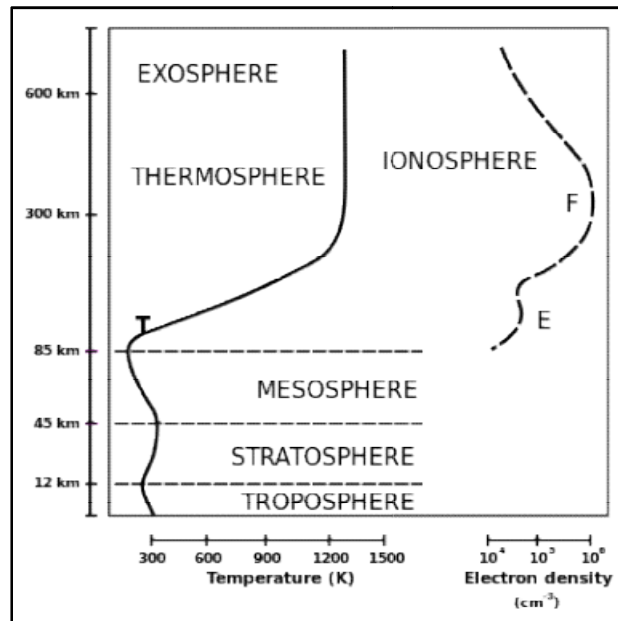
a) D-Region: The region between about 75 and 95km above the Earth in which the (relatively weak) ionization is mainly responsible for absorption of high-frequency radio waves.

b) E-Region: The region between about 95 and 150km above the Earth that marks the height of the regular daytime E-layer. Other subdivisions, isolating separate layers of irregular occurrence within this region, are also labeled with an E prefix, such as the thick layer, E2, and a highly variable thin layer, Sporadic E. Ions in this region are mainly O₂⁺.

c) F-Region: The region above about 150km in which the important reflecting layer, F₂, is found. Other layers in this region are also described using the prefix F, such as a temperate-latitude regular stratification, F₁, and a low-latitude, semi-

regular stratification, F1.5. Ions in the lower part of the F-layer are mainly NO^+ and are predominantly O^+ in the upper part. The F-layer is the region of primary interest to radio communications.

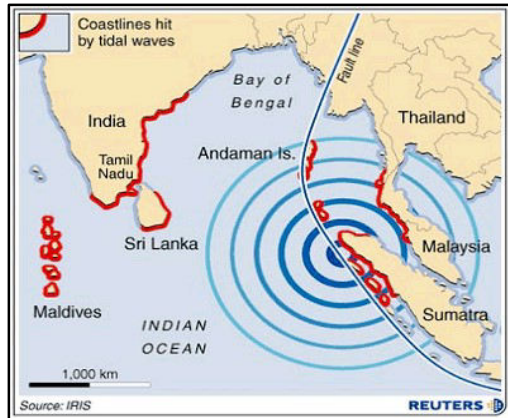
d) Topside: This part of the Ionosphere starts at the height of the maximum density of the F2 layer of the Ionosphere and extends upward with decreasing density to a transition height where O^+ ions become less numerous than H^+ and He^+ . The transition height varies but seldom drops below 500km at night or 800km in the daytime, although it may lie as high as 1100km. Above the transition height, the weak ionization has little influence on radio signals.



TSUNAMI AND GRAVITY WAVE CHARACTERISTICS

The possibility of tsunami detection by the way of coupled atmospheric gravity waves has been proposed by Peltier & Hines (1976). They mainly discussed how the vertical displacement of the sea surface due to a tsunami can be a source of gravity waves in the atmosphere. The gravity wave created at the sea surface propagates obliquely upward. Due to the exponential decrease of density with altitude, conservation of kinetic energy causes an exponential increase in the wave amplitude. As it reaches the ionosphere, the gravity wave should then perturb the local plasma, and induce some detectable signals on radio sounding.

Tsunami are non-dispersive waves; their propagation velocity v is obtained from shallow-water equations and depends on gravity g and water depth d as $v = \sqrt{gd}$. If we take the values $g = 9.8 \text{ m/s}^2$ and $d = 5000 \text{ m}$, this velocity is $v = 221 \text{ m/s}$. Typical period range is between 10 and 30 min (600–1800 s). Thus Tsunami waves have long period and long wavelength.



On December 26, 2004, at 00:58:53 UT, a strong earthquake ($M_w = 9.15$) originated in the Indian Ocean just north of Simeulue island, off the western coast of northern Sumatra, Indonesia (Park *et al.*, 2005). This earthquake generated Tsunami that was among the deadliest disasters in modern history. The hypocenter of the quake was $3.31^\circ\text{N}, 95.85^\circ\text{E}$, some 160 km west of Sumatra at a depth of 30 km below the mean sea level. The epicenter of the quake was 3.29°N and 95.94°E . An estimated 1200 km of fault line slipped about 15 meter along the subduction zone, where the Indian Plate dives under the Burma Plate. Due to the sideways movement between the plates, the seabed is estimated to have risen by several meters, displacing an estimated 30 km^3 of water and triggering Tsunami waves.

GRAVITY WAVE SIGNATURE IN THE IONOSPHERE

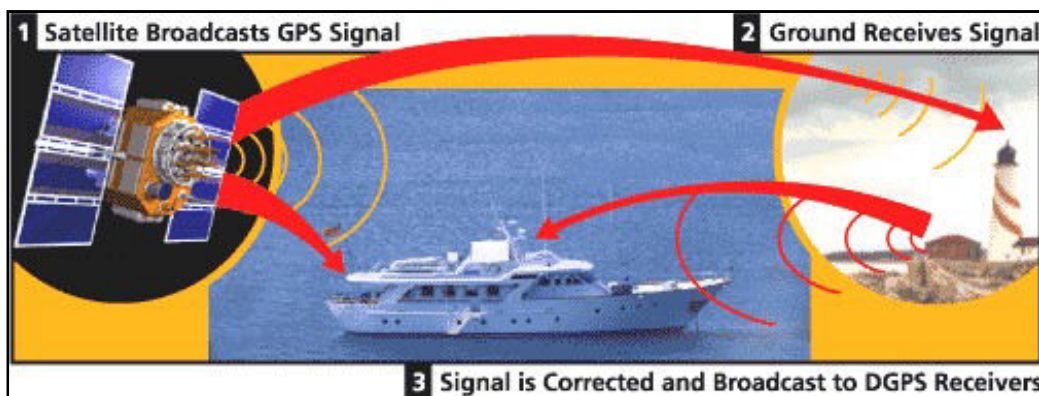
As the gravity waves propagates upward, it will interact with the ionospheric plasma through different mechanisms. Some early works extended Hines's formalism to ionospheric heights, including the effect of the Lorentz force due to the magnetic field, and the ions-neutral particles collision terms. This gravity wave-ionosphere interaction is one of the main sources of Travelling Ionospheric Disturbances. TIDs are commonly observed in the ionosphere, in a wide range of wavelength and frequency. Several studies have described the different types of TIDs usually found, and developed models of gravity waves-ionosphere coupling (Clark *et al.* 1971). However, most TIDs have periods longer than 1 hour and larger scales than what a tsunami gravity wave is likely to present.

INTRODUCTION TO GPS

The Global Positioning System (GPS) is a satellite-based navigation system made up of a network of 24 satellites placed into orbit by the U.S. Department of Defense. GPS was originally intended for military applications, but in the 1980s, the government made the system available for civilian use. GPS works in any weather conditions, anywhere in the world, 24 hours a day. There are no subscription fees or setup charges to use GPS.

GPS satellites circle the earth twice a day in a very precise orbit and transmit signal information to earth. GPS receivers take this information and use triangulation to calculate the user's exact location. Essentially, the GPS receiver compares the time a signal was transmitted by a satellite with the time it was received. The time difference tells the GPS receiver how far away the satellite is. Now, with distance measurements from a few more satellites, the receiver can determine the user's position and display it on the unit's electronic map.

A GPS receiver must be locked on to the signal of at least three satellites to calculate a 2D position (latitude and longitude) and track movement. With four or more satellites in view, the receiver can determine the user's 3D position (latitude, longitude and altitude). Once the user's position has been determined, the GPS unit can calculate other information, such as speed, bearing, track, trip distance, distance to destination, sunrise and sunset time and more.



The Global Positioning Satellites (GPS) broadcast at two different frequencies which are L1 and L2 frequency. This allows positional measurements to be

corrected for ionospheric effects. Alternately, information about the ionosphere can be derived.

INTRODUCTION TO TEC IN IONOSPHERE

The total electron content (TEC) is a measure of the total amount of electrons along a particular line of sight. Units of TEC are 10^{12} electrons per square centimeter. The ionospheric delay is a function of the Total Electron Content (TEC) along the signal path and the frequency of the propagating signals. Since the ionosphere is a dispersive medium for radio waves, a dual-frequency GPS receiver can minimize ionospheric delay through a linear combination of L1 and L2 observables. The total electron content (TEC) is a measure of the total amount of electrons along a particular line of sight. The dual frequency signals of GPS at an altitude of 20,200km allow the measurement of the total number of free electrons, along ray path from GPS satellite to receiver. This TEC, however usually includes instrumental biases inherent in the GPS receivers and transmitters. These biases must be removed to obtain absolute values of TEC.

The ionosphere is a shell of electrons and electrically charged atoms and molecules that surrounds the earth, stretching from a height of about 50 km to more than 1000 km above the earth's surface. The existence of the ionosphere is primarily due to the extreme ultraviolet radiation and X-rays from the sun. Each regions of the ionosphere are produced by varies kind of chemical species.

ESTIMATION OF TEC

The estimation of Total Electron Content (TEC) using a dual frequency GPS receiver is made possible by the dispersive nature of the ionized medium between the GPS satellites and a GPS receiver on the ground. Since the ionosphere and plasma sphere are weakly ionized plasmas, both contribute to the TEC that is measured using a GPS receiver. In this report, however, we consider only the ionosphere and acknowledge that both the estimated receiver bias and the calibrated TEC we compute contain implicit contributions from the plasma sphere. The ionosphere, being a weakly ionized plasma, imparts a group delay (Δt) and carrier phase advance to an RF signal that, to first order, are equal in

magnitude, opposite in sign, and proportional to the total number of electrons encountered along the line of sight (LOS):

$$\Delta t = 40.30 \text{ TEC} / (cf^2)$$

where f is the frequency of the signal in Hertz and c is the speed of light in m/s. By measuring the group delay or carrier phase advance imparted by the ionosphere on the two GPS carrier signals, L1 ($f_1 = 1575.42$ MHz) and L2 ($f_2 = 1227.60$ MHz), the TEC encountered along the signal propagation path may be inferred. In practice, complications arise due to hardware timing biases and cycle slips, which are breaks in the measured phase.

One estimate of the TEC along the LOS to each GPS satellite may be obtained in terms of the pseudorange measurements on the L1 and L2 frequencies as follows:

$$\text{TEC}_p = A \{ [P_2 - P_1] - [BR + BS] + D_p + E_p \}$$

Where,

P_1 is the pseudorange on L1 (ns)

P_2 is the pseudorange on L2 (ns)

BR is the receiver differential code bias (ns)

BS is the satellite differential code bias (ns)

D_p is the differential pseudorange multipath error (ns)

E_p is the differential pseudorange measurement noise (ns)

The constants A and B that give TEC_p in units of TECU (where 1 TECU = 10^{16} el/m²) are:

$$A = 2.854 \text{ TECU/ns}$$

$$B = 1.812 \text{ TECU/L1 cycle}$$

Measuring the TEC using the pseudoranges involves determination of the hardware differential code biases, BR and BS, and subtracting them from the differential pseudorange measurement. Accuracy in the measurement of TEC using the pseudoranges alone, however, is limited by the multipath and measurement noise terms which are difficult to model and can exceed those of

the phases by an order of magnitude or more. We note that the receiver bias, BR, is alternatively referred to as the “station” bias because this contribution to the delay generally depends on the antenna and cable configuration in addition to the receiver hardware itself. An alternative way to estimate the TEC along the LOS to each satellite involves the carrier phases on the L₁ and L₂ frequencies as follows:

$$TEC_L = B \{ [L_1 - (f_1/f_2) L_2] - [N_1 - (f_1/f_2) N_2] + DL + EL \}$$

Where,

L₁ is the carrier phase on L1 (cycles)

L₂ is the carrier phase on L2 (cycles)

N₁ is the integer ambiguity of L1 phase (cycles)

N₂ is the integer ambiguity of L2 phase (cycles)

DL is the differential phase multipath error (cycles)

EL is the differential phase measurement noise (cycles)

Measuring the TEC using the carrier phases is generally more precise in that multipath error and measurement noise are smaller and may generally be neglected. The disadvantage is that the integer numbers of accumulated cycles of phase for each frequency, N₁ and N₂, are unknown and change (often dramatically) after each cycle slip.

Standard practice for estimating the TEC using a dual frequency GPS receiver combines the strengths of both the pseudorange and carrier phase approaches. The calculation performed by GPS in real time is based on the phase formulation with the multipath and noise terms neglected, while the pseudoranges are used to estimate the unknown number of accumulated phase cycles. The method proceeds by defining the calibrated TEC, as equal to the relative total electron content, TEC_R, minus the satellite and receiver differential code biases:

$$TEC = TEC_R - A (BR + BS)$$

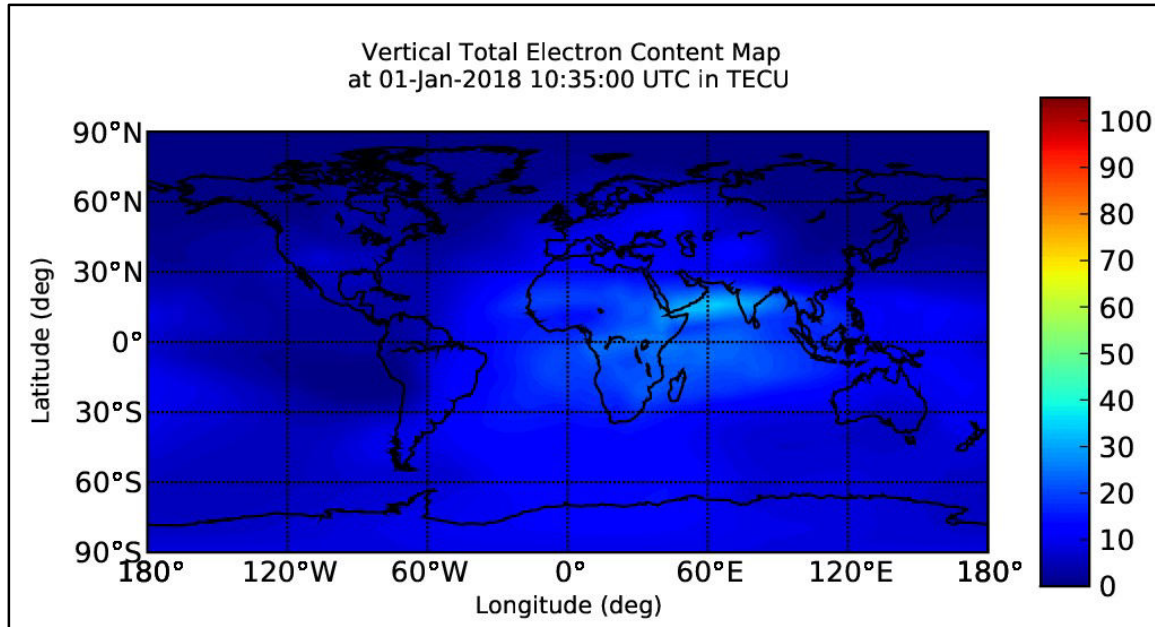


Fig. IARS Website (Ionospheric and Atmospheric Remote sensing)

DATA

On December 26, 2004, at 00:58:53 UT, a strong earthquake ($M_w = 9.15$) originated in the Indian Ocean. The hypocenter of the quake was 3.31°N , 95.85°E , some 160 km west of Sumatra at a depth of 30 km below the mean sea level. The epicenter of the quake was 3.29°N and 95.94°E . An estimated 1200 km of fault line slipped about 15 meter along the subduction zone.

We choose 8 stations to study the case study:-

Station	Lat	Lon
Aizwal	23.83	92.62
Bagdodra	26.68	88.32
Bangalore	12.95	76.68
Guwahati	26.12	91.59
Hyderabad	17.44	78.37
Kolkata	22.64	88.44
Trivandrum	8.47	76.91
Vizag	17.68	83.21

The plots of the studied stations are:-



METHODOLOGY

PHASE I: Acquisition and Processing of Data

To implement Satellite Based Augmentation System(SBAS) of GPS in India, Indian Space Research Organisation(ISRO) in collaboration with Airport Authority of India(AAI) has set up 20 GPS receivers at the different airports all over India. The dual frequency GPS receivers, operating at L1 (1575.42 MHz) and L2 (1227.6 MHz) frequencies measure the Total Electron Content along the slant ray path (STEC). The data contains STEC, as well as the azimuth, elevation, satellite PRN Number, time etc at 1 minute interval in RINEX format (Mannucci *et al.*, 1997). In Addition to RINEX format we have ASCII Data which is user friendly.By measuring the carrier phase at the two frequencies the STEC is obtained (Klobuchar, 1996) along the path from satellite to the receiver. The 350 km sub ionospheric point of the satellite signal is calculated from the station's location, azimuth and elevation data.

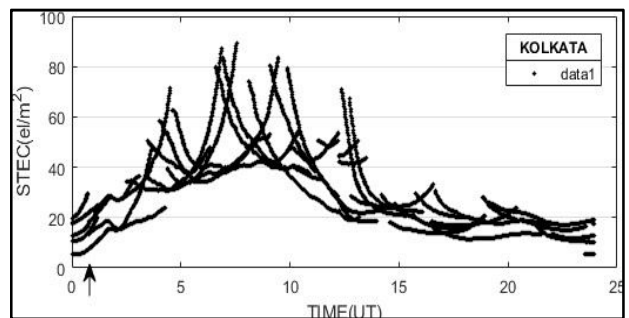
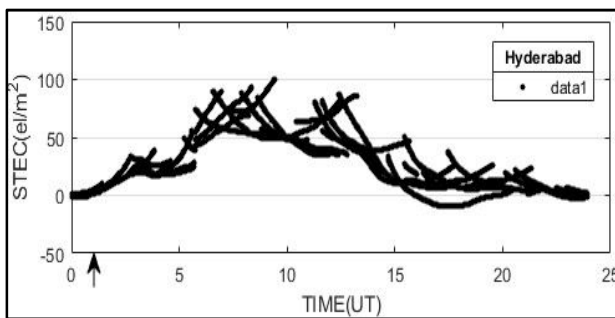
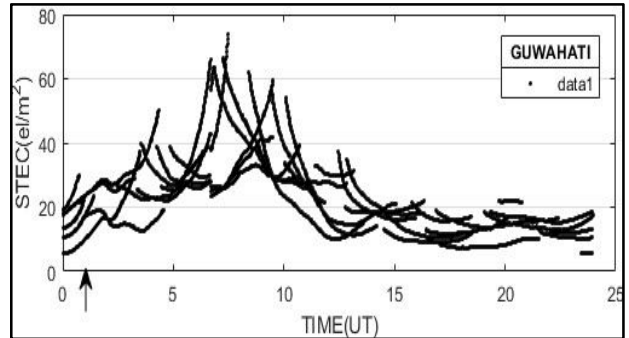
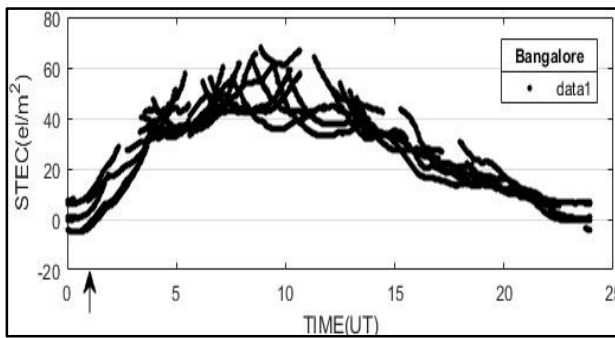
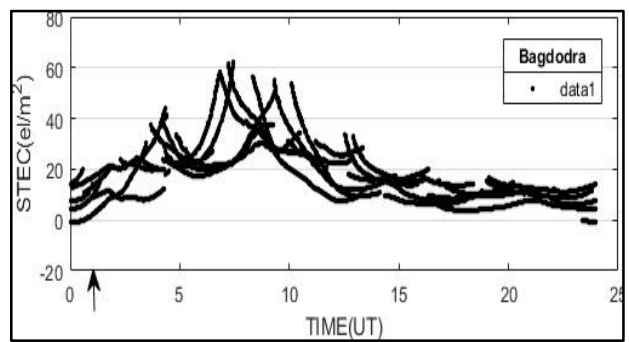
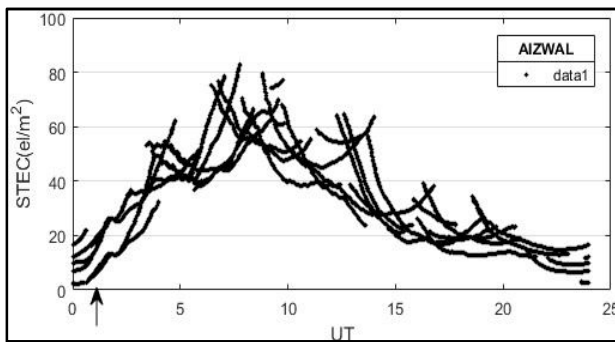
PHASE II: ANALYSIS OF DATA

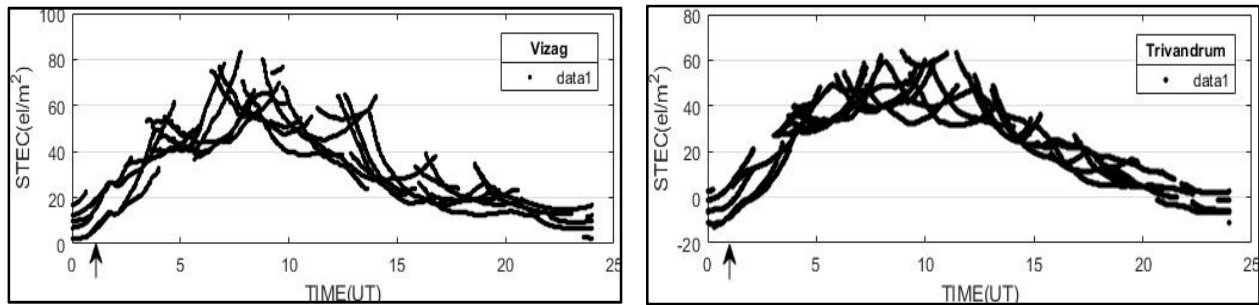
Data analysis was carried out in MATLAB as a plot of Time and TEC variation.

- The raw data was plotted for PRN 3 satellite data. In this we plot slant TEC vs Universal time(UT)

```
ele=ele1(find((azim1>=0)&(ele1>=x)));  
azim=azim1(find((azim1>=0)&(ele1>=x)));  
s4t=s41(find((azim1>=0)&(ele1>=x)));  
stec=tecl(find((azim1>=0)&(ele1>=x)));
```

```
plot(time,stec,'*');
```





Figs. The **diurnal variation of STEC** at different stations on December 26, 2004. The different curves show TEC along the slant path for different satellites. The large scatter of the plots may be attributed to the differing look angles of the GPS satellites and transmitter and receiver biases. The low value of TEC (approximately 0 TEC unit) around 00:00 UT may be receiver bias error. The diurnal minimum normally lies in the 2–10 TEC unit range in the pre sunrise hour. The **arrow** indicates the commencement of the earthquake.

- The following code was written to plot the TEC variation recorded by various stations and also the scintillations.

```

test_prn=prn1(find(diff(prn1)~=0))
for i=1:length(test_prn)
tec2=tec1(find(prn1==test_prn(i)));
s42=s41(find(prn1==test_prn(i)));
time2=time1(find(prn1==test_prn(i)));
prn2=prn1(find(prn1==test_prn(i)));
lat2=lat1(find(prn1==test_prn(i)));
lon2=lon1(find(prn1==test_prn(i)));
[sri1,sri2]=find((time2>=0)&(time2<=24))
if(sri1~=0)
time22=time2(sri1(1))
tec22=tec2(sri1(1))
s422=s42(sri1(1))

test=diff(tec2);
[t1,t2]=find(abs(diff(time2))>0.05);
att=[1 t1' length(tec2)]

```

We got the following plot:-

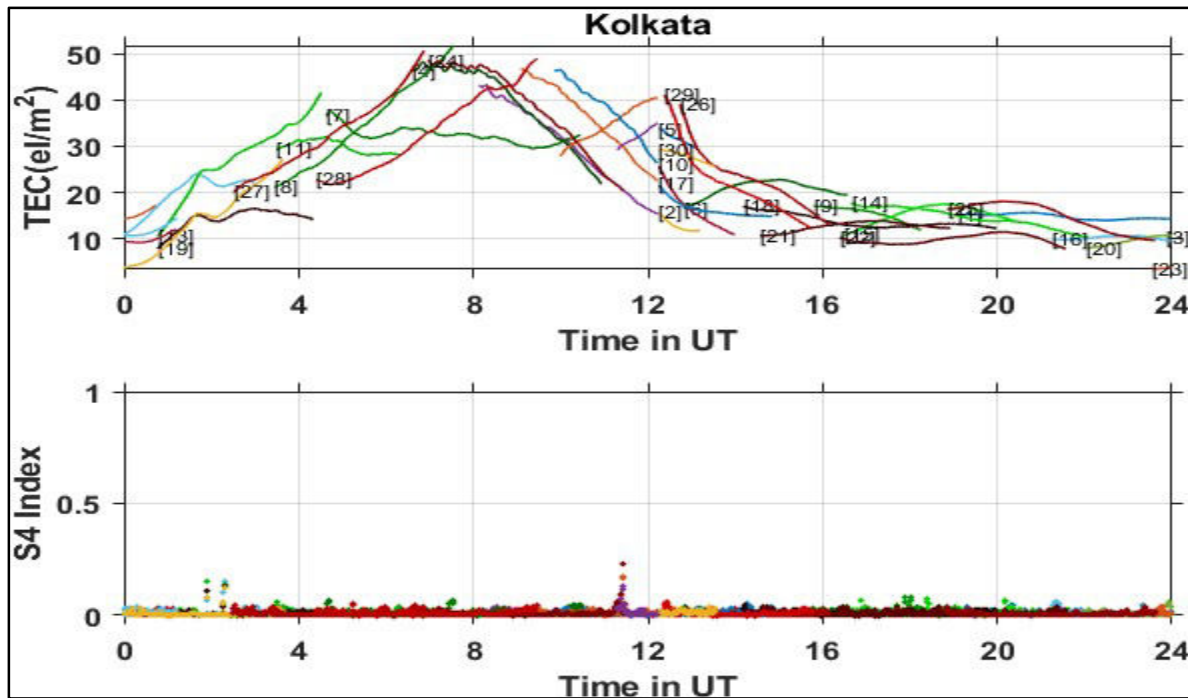


Fig:-Plot between STEC variation at different time recorded at various PRN. Second graph shows plot between scintillation index and time.

- The following code was written to find the detrending STEC curve and then we measure delta_tec which is STEC - MEAN STEC

```

stec1=stec(find(prn==3) & (time<=10))
time1=time(find(prn==3) & (time<=10))

stec11=runmean(stec1,10);
subplot(2,2,1)
plot(time1,stec1,'b*');hold on;
plot(time1,stec11,'r*');hold on;
legend('stec','mean stec');
subplot(2,2,3)
plot(time1,stec1-stec11,'g*');hold on;
legend('delta tec');
delta_tec=stec1-stec11;

```

The plot was like this:-

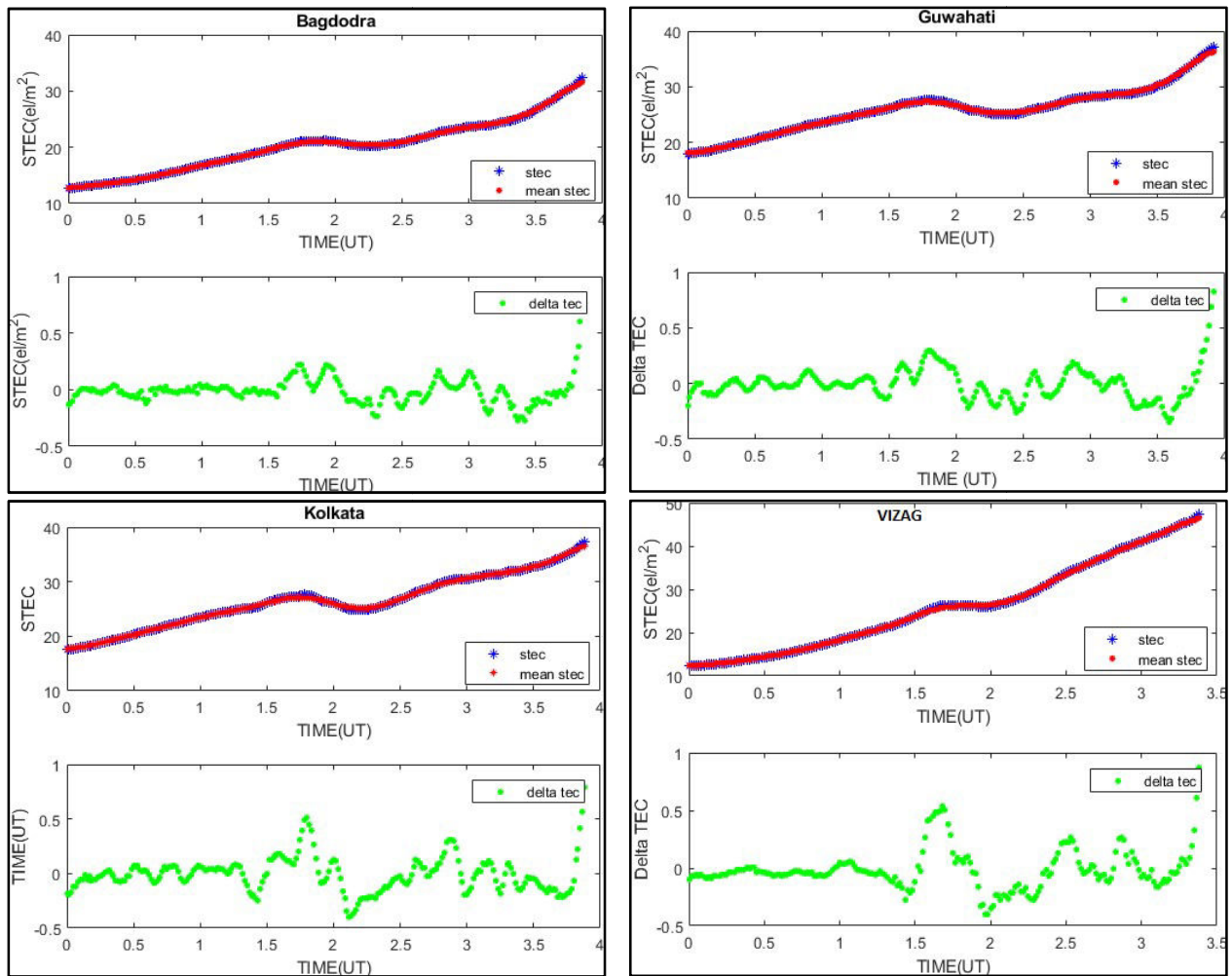


Fig.- Variation of STEC at 4 stations. The red curve is detrended curve and the green curve is the delta TEC variation.

RESULT AND DISCUSSION

We studied the ionospheric effects observed on the Slant Total Electron Content along the ray path from different stations near the east coast of the Indian subcontinent subsequent to the Sumatra-Andaman earthquake of December 26, 2004. The Sumatra Earthquake caused Tsunami which generated gravity waves. These waves travel slower and hence would take approximately 45 minutes to 1 hour to arrive. A significant perturbation of the TEC (+0.5 to -0.5 units of TEC) approximately 45 minutes after the earthquake was recorded on a number of satellites from stations like Vizag, Hyderabad, Kolkata, Bagdogra, Guwahati, and Aizwal. Although ionospheric perturbations we studied are mainly attributed to seismic activities, the mechanism of coupling of the ionosphere to earthquake is yet to be fully understood. Also it is assumed that as we move away from the epicenter there is a delay in response. From the obtained plot it is evident that there is diminishing of amplitude with increase in distance from epicenter.

CONCLUSION

It is known that sudden vertical displacement or tilting of earth's surface near the epicenter of the earthquake can generate seismic airwaves. It has also been observed that the pressure waves propagating in the atmosphere after natural events such as tsunami, volcanic eruption and meteoritic impacts observed global atmospheric perturbations.

Extending analysis to include the ionosphere will help detect signals that are potentially useful for analysis of Solid earth processes.

REFERENCES-

- Lay, T., et al. (2005), The great Sumatra-Andaman earthquake of 26 December 2004, *Science*, 308, 1127–1133.
- Mala.S,et al. (2017) Origin of the ahead of tsunami traveling ionospheric disturbances during Sumatra tsunami and offshore forecasting.
- A.Dasgupta,et al.(2006)Ionospheric perturbations observed by the GPS following the December 26th,2004 Sumatra-Andaman earthquake.
- Infrasonic monitoring for atmospheric studies by A.LePichon
- Mai, C.-L. and J.-F. Kiang, Modeling of ionospheric perturbation by 2004 Sumatra tsunami, *Radio Sci.*,
- GPS SCINDA: A Real Time GPS Data Acquisition And Ionospheric Analysis System for SCINDIA